PAPER

Remarkably high surface visco-elasticity of adsorption layers of triterpenoid saponins

Konstantin Golemanov,[a] Slavka Tcholakova,[*b] Nikolai Denkov,[b] Edward Pelan[a] and Simeon D. Stoyanov[acd]

Saponins are natural surfactants, with molecules composed of a hydrophobic steroid or triterpenoid group, and one or several hydrophilic oligosaccharide chains attached to this group. Saponins are used in cosmetic, food and pharmaceutical products, due to their excellent ability to stabilize emulsions and foams, and to solubilize bulky hydrophobic molecules. The foam and emulsion applications call for a better understanding of the surface properties of saponin adsorption layers, including their rheological properties. Of particular interest is the relation between the molecular structure of the various saponins and their surface properties. Here, we study a series of eight triterpenoid and three steroid saponins, with different numbers of oligosaccharide chains. The surface rheological properties of adsorption layers at the air–water interface, subjected to creep-recovery and oscillatory shear deformations, are investigated. The experiments showed that all steroid saponins exhibited no shear elasticity and had negligible surface viscosity. In contrast, most of the triterpenoid saponins showed complex visco-elastic behavior with extremely high elastic modulus (up to 1100 mN m^{-1}) and viscosity (130 N s m^{-1}). Although the magnitude of the surface modulus differed significantly for the various saponins, they all shared qualitatively similar rheological properties: (1) the elastic modulus was much higher than the viscous one. (2) Up to a certain critical value of surface stress, τ_C, the single master curve described the dependence of the creep compliance *versus* time. This rheological response was described well by the compound Voigt model. (3) On increasing the surface stress above τ_C, the compliance decreased with the applied stress, and eventually, all layers became purely viscous, indicating a loss in the layer structure, responsible for the elastic properties. The saponin extracts, showing the highest elastic moduli, were those of Escin, Tea saponins and Berry saponins, all containing predominantly monodesmosidic triterpenoid saponins. Similarly, a high surface modulus was measured for Ginsenosides extracts, containing bidesmosidic triterpenoid saponins with short sugar chains.

1 Introduction

Saponins are a class of natural surfactants found in more than 500 plant species.[1–3] They consist of a hydrophobic head group, called aglycone, with one or several hydrophilic oligosaccharide (sugar) chains connected to the aglycone *via* glycoside bonds. The term "saponin" includes a great variety of compounds, differing both in structure and in sugar composition. The saponins are classified on the basis of: (i) the type of aglycone (triterpenoid or steroid) and (ii) the number of sugar chains attached to it. The most common saponins have two sugar chains (bidesmosidic type), some have one sugar chain (monodesmosidic type) and in rare cases three sugar chains. Triterpenoid saponins are more proliferated in nature than steroid saponins.

Saponins exhibit a number of non-trivial biological effects, such as anti-inflammatory,[4] anti-fungal, anti-bacterial, anti-yeast,[5] cholesterol-lowering,[6] anti-cancer,[7] and adjuvant effects,[8] which are currently under active investigation.[1]

Due to the amphiphilic structure of their molecules, many saponins have strong surface activity. Several authors[9–15] reported high surface elasticities of saponin adsorption layers at the air–water interface, in both dilatation[9,14] and shear deformations.[10–13,15] These properties are important in the context of the saponin applications as foam and emulsion stabilizers. It was found that surfactants with higher surface moduli decrease the rate of bubble Ostwald ripening[16–19] and liquid drainage in foams.[16,20] In some studies, positive correlation was reported between foam stability and the higher surface elasticity or surface viscosity.[21,22] Therefore, saponins with high surface moduli are expected to produce more stable foams. In addition,

[a]*Unilever R&D, Vlaardingen, The Netherlands*

[b]*Department of Chemical Engineering, Faculty of Chemistry and Pharmacy, Sofia University, 1 J. Bourchier Ave., 1164 Sofia, Bulgaria. E-mail: SC@LCPE.UNI-SOFIA.BG; Fax: +359 2 962 5643; Tel: +359 2 962 5310*

[c]*Laboratory of Physical Chemistry and Colloid Science, Wageningen University, 6703 HB Wageningen, The Netherlands*

[d]*Department of Mechanical Engineering, University College London, Torrington Place, London WC1E 7JE, UK*

the surface rheological properties were shown to affect dynamic foam properties, such as foam viscosity and bubble-wall friction,[16,23] as well as bubble rearrangement in static foams.[24,25] Therefore, the high surface moduli, exhibited by some saponins, make them very prospective foam stabilizers. Other systems which show promise in this respect are the hydrophobins[26,27] and hydrophobic solid particles.[28–30] Due to their non-trivial surface rheological behavior, all these systems attract currently a lot of research interest.

In our previous study,[13] we showed that the rheological behavior of adsorption layers of saponins, extracted form *Quillaja saponaria* Molina (of triterpenoid type) and *Yucca schidigera* (of steroid type), was very different – see Table 1 and Fig. 1 for the molecular structures of the saponins studied here. When subjected to creep-recovery shear deformation, the adsorption layers of Quillaja saponins (QS) exhibited a complex viscoelastic behavior with significant shear elasticity ($\approx 30 \div 40$ mN m^{-1}). This rheological behavior was described well by the compound Voigt (CV) model, containing two Kelvin and one Maxwell elements, connected sequentially. In contrast, the adsorption layers of Yucca saponins (YS) had negligible surface shear elasticity and very low surface viscosity, η_S.

To explain qualitatively the big difference between the rheological response of QS and YS, we invoked the physical picture in ref. 13. High shear modulus, G, of the adsorption layer was attributed to dense packing and strong lateral interaction between the molecules in the adsorption layers. In the case of saponins, such interactions could be the hydrogen bonds between the oligosaccharide chains in the neighboring molecules in the adsorption layer. Appropriate structure and/or conformation of the saponin molecule could promote denser packing and favorable mutual orientation of the oligosaccharide chains, thus allowing the formation of stronger hydrogen bonds – see Fig. 2 for a schematic presentation of the possible orientations of the saponin molecules in the adsorption layers. In this way, the structure of the saponin molecules could be related (qualitatively) to a certain type of rheological behavior.

The most important structural difference between the QS and YS molecules is the type of aglycone. QS is a triterpenoid saponin, whereas YS is a steroid saponin. A similar difference between the surface moduli of steroid and triterpenoid saponins was noticed previously by Joos *et al.*[11] who tested the triterpenoid saponin Senegin, isolated from *Polygala senega* L.[31] and the steroid saponin Digitonin. These authors detected a measurable yield stress for the triterpenoid Senegin layers, while no yield stress and much lower viscosity were observed for the steroid Digitonin layers. Based on these studies,[9,11,13] one may speculate that the adsorption layers from the molecules of triterpenoid type pack better and lead to higher surface shear modulus. However, a more systematic set of data is needed, with a much wider pool of saponin types, to draw more definitive conclusions.

Table 1 Studied saponins. The molecular structures (A)–(E) are shown in Fig. 1. The critical micelle concentrations (CMC) were determined by measuring the surface tension isotherms and are presented as weight concentration of saponin in the solution

Type of aglycone	Molecular structure	Trade name	Abbreviation used in text	Plant species	Extracted from	Supplier	Concentration of saponin, wt%	References	CMC, wt% saponin
Triterpenoid	A	Horse chestnut extract	HC	*Aesculus hippocastanum*	Seeds	Xi'an Biof Bio-technology Co., Ltd	20	4	0.146
	A	Escin	ES	*Aesculus hippocastanum*	Seeds	Sigma	≥95	4	0.008
	A	Glycyrrhizic acid ammonium salt	LIC	*Glycyrrhiza glabra*	Roots	Sigma	≥95	—	Not measured
	A + B	Tea Saponin	TS	*Camelia oleifera* Abel	Seeds	Zhejiang Yuhong Import & Export Co., Ltd	96.2	32	0.017
	A + B	Berry Saponin Concentrate	BSC	*Sapindus mukurossi*	Fruits	Ecological Surfactants, LLC	53	33	≈0.1
	A + B	Sapindin	SAP	*Sapindus trifoliatus*	Fruits	Sabinsa Corporation	50	33 and 34	≈ 0.03
	B	Quillaja Dry 100, Non-preserved	QD	*Quillaja saponaria* Molina	Bark	Desert King, Chilie	25.6	35	0.025
	C	Ginsenosides	GS	*Panax ginseng*	Roots	Xianyang Hua Yue Biol. Engin. Co., Ltd.	80	7,36,37	0.019
	—	Ayurvedic Saponin Concentrate	ASC	*Acacia concinna*	Pods	Ecological Surfactants, LLC	30	38–40	≈0.3
Steroid	D + E	*Tribulus terrestris* extract	TT	*Tribulus terrestris*	Herb	Sabinsa Corporation	45	41 and 42	0.048
	D + E	Foamation Dry 50	FD	*Yucca schidigera*	—	Desert King, Chilie	9	5 and 43	≈0.03
	E	Fenusterols®	FS	*Trigonella foenum-graecum*	Seeds	Sabinsa Corporation	50	44 and 45	0.089
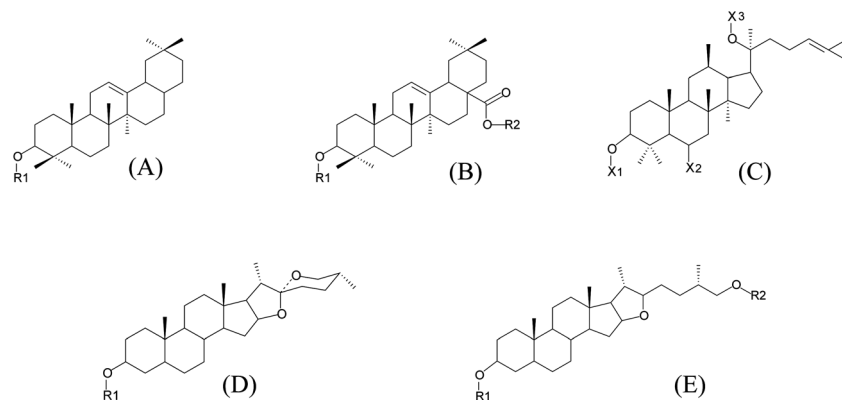
Fig. 1 Structure of the saponins in the studied extracts. R1–R2 and X1–X3 designate sugar chains with different lengths and/or compositions; X1–X3 can also designate a H atom. (A) Monodesmosidic and (B) bidesmosidic triterpenoids with oleanane type of aglycone. (C) Mono- or bidesmosidic triterpenoids with dammarane type of aglycone. Steroid saponins of (D) spirostanol and (E) furastanol type.
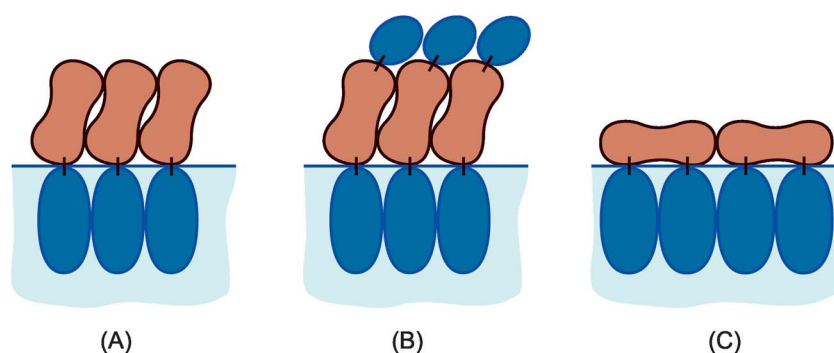
Fig. 2 Schematic presentation of the possible structure of the adsorption layers for: (A) monodesmosidic triterpenoid saponins, such as Escin; (B) bidesmosidic triterpenoid saponins in a side-on configuration, such as GS; (C) bidesmosidic triterpenoid saponins in a lay-on configuration, such as QD. The side-on configurations (A) and (B) correspond to an area per molecule of 0.4 to 0.5 nm^2, as determined from surface tension isotherms, and extremely high surface elasticity and viscosity, whereas the lay-on configuration in (C) is characterized with an area per molecule larger than 1 nm^2 and lower (but still very high) surface elasticity and viscosity. The high elastic and viscous moduli are probably caused by strong hydrogen bonds between the oligosaccharide chains (shown in dark blue) in the neighboring adsorbed molecules. The brown blobs represent the hydrophobic scaffolds of the saponin molecules.

The main purpose of the current study is to investigate further the surface rheological properties of the various saponin types and to deepen our understanding of the potential structure–behavior relation. A comparative study is conducted with twelve saponin extracts which differ significantly in their molecular structure – both in the type of aglycone and in the number of oligosaccharide chains. We tested eight triterpenoid and three steroid saponins, with different numbers of the sugar chains. Adsorption layers at the air–water interface were studied, in creep-recovery and oscillatory shear deformation. Three major tasks were defined:

(1) To characterize the rheological response of the saponin adsorption layers, including the effects of time of layer aging, shear stress, and strain amplitude.

(2) To describe the observed visco-elastic response of some of the saponin layers by an appropriate rheological model.

(3) To search for a possible correlation between the rheological behaviour of the adsorption layers and the molecular structure of the saponins.

The article is organized as follows. The used materials and methods are described in Section 2. Section 3 presents the experimental results and their discussion. Section 4 summarizes the main results and conclusions.

2 Materials and methods

2.1 Materials

Table 1 provides information about all saponins studied: trade name, abbreviation used in the text, supplier, origin of the plant extract, part of the plant which was processed, concentration of saponins in each extract, references containing information about the chemical composition of these extracts, and the critical micelle concentration (CMC) as determined by us from surface tension isotherms, measured by the Wilhelmy plate method on a K100 instrument of Krüss GmbH, Germany.

Fig. 1 presents the basic molecular structures of these saponins. The aglycones depicted in Fig. 1A and B are triterpenoid, from the oleanane type.[2] The oligosaccharide chain of the monodesmosidic triterpenoid saponins is connected to

the aglycone *via* an ether bond, as shown in Fig. 1A. The same bond is present in the bidesmosides, with an additional oligo-saccharide chain, connected *via* an ester link, as shown in Fig. 1B. Besides the sugar chains, other chemical groups could be attached to the aglycone: OH, COOH, CH_3, CH_2OH. The aglycone in Fig. 1C is again triterpenoid but of dammarane type.[2] All triterpenoid saponins studied here contain oleanane aglycone, except for GS (extract of *Panax ginseng*) which contains dammarane aglycone and is a mixture of mono- and bidesmo-sides, the bidesmosides being predominant.[36]

It is important to note that only two of the studied plant extracts contain pure saponin components. Both are products of Sigma: Escin (ES), also known as Aescin (cat. num. E1378, CAS Number 6805-41-0, molecular formula $C_{54}H_{84}O_{23}$), and glycyrrhizic acid ammonium salt (abbreviated as LIC in the current paper, cat. num. 50531, CAS number 53956-04-0, molecular formula $C_{42}H_{65}NO_{16}$). The other samples are crude plant extracts, containing a complex mixture of different components. The given plant extract contains a variety of saponin molecules, which share the same type of aglycone. The oligosaccharide chains in the given saponin extract can differ in their number, length and composition (type of sugar residues). HC is a crude extract from horse chestnut (*Aesculus hippo-castanum*) which contains Escin as an active component.

The saponins presented in Fig. 1D and E belong to the steroid class, and are of spirostanol or furastanol type, respectively. Spirostanols have one sugar chain, while furastanols have two. Detailed information on the structure and classification of various saponins can be found in the review.[2]

The experiments were performed with solutions of 0.5 wt% saponin and 10 mM NaCl. This saponin concentration is much higher than the critical micelle concentrations (CMC) of the studied saponins. NaCl was added as a neutral electrolyte to all solutions in order to ensure well defined ionic strength during the experiments.

2.2 Methods

The surface rheological properties were characterized by a double-wall ring geometry (DWRG),[46,47] attached to a ARG2 rotational rheometer (TA Instruments). This set-up represents a circular channel, carved into a disk (made of delrin), which in turn is fitted to a Peltier plate. The ring is made of a Pt/Ir alloy and has a diamond cross-section. The ring is positioned on the water–air interface, in the center of the channel. The channel and a small vessel, filled with water, are covered with a circular plastic cell to saturate the air and suppress water evaporation from the solution surface.

The rheometer provides information for the angle of rotation of the tool, Ω, and the torque, M, exerted on the tool. From these data and from the geometrical parameters of the setup, the surface stress and the layer deformation can be calculated. In the general case, one has to also account for the coupling between the flows on the surface and the sub-surface layers[46] and the raw data for the torque could be corrected by using a numerical procedure.[46] However, if the adsorption layer has high surface viscosity, η_S, and the Boussinesq number, Bo $\gg$ 1,

the analysis is greatly simplified. By definition, the Boussinesq number represents the ratio between the surface and sub-surface drags:[48]

$$\text{Bo} = \frac{\eta_S (V/L_S) P_S}{\eta (V/L_B) A_S} = \frac{\eta_S}{\eta Q} \tag{1}$$

where η is bulk viscosity, V is characteristic flow velocity, and L_S and L_B are characteristic length scales over which the surface and sub-surface flows decay. P_S is the perimeter of the geometry in contact with the interface, A_S is the area of the geometry in contact with the solution, and Q is a geometrical parameter.

As shown previously,[46] at Bo $\gg$ 1, the torque originates almost exclusively from the contribution of the surface stress, and the raw data need no special corrections. In most of the experiments presented in the current paper, Bo > 1000. In such cases, taking into account that the DWR configuration is a 2D-analog of the double-wall rheometer,[47] one can calculate the strain, γ, and stress, τ, *via* the relations:[47]

$$\gamma = \frac{\Omega}{\left(\frac{R_2}{R_1}\right)^2 - 1} + \frac{\Omega}{1 - \left(\frac{R_3}{R_4}\right)^2} \tag{2}$$

$$\tau = \frac{M}{2\pi \left(R_2{}^2 + R_3{}^2\right)} \tag{3}$$

here, R_2 and R_3 are the inner and outer radii of the ring, while R_1 and R_4 are the inner and outer radii of the circular channel, respectively.

We subjected the saponin layers to several rheological tests in oscillatory (amplitude or frequency sweep) and creep-recovery shear deformations. All experiments were performed at 20 °C. Care was taken to remove all bubbles from the solution surface. Before each experiment, the studied adsorption layer was pre-sheared for 3 min at a shear rate of 170 s^{-1} (18 rad s^{-1}). Next, the layer was left to age for a certain period (30 min in most experiments) and the actual rheological measurements were performed. In several control experiments, the experimental protocol included an extra initial step of equilibrating the layer for 1 hour (no deformation applied) before the pre-shear. This step was applied to allow for maximal adsorption in the layer before starting any deformation. The experiments with and without this initial adsorption step yielded the same results, and therefore, this step was not included in the standard procedure.

In the amplitude sweep test, we varied the strain amplitude, γ_A, from 0.01 to 20% at constant frequency, ω, which was fixed at 1 Hz. In the creep-recovery experiments, we applied constant stress for a given creep time, t_{CR}, and afterwards, we monitored the relaxation of the deformation for 30 min. Experiments at $t_{CR} = 100$ s and at different values of the shear stress were performed.

The performed experiments showed that the surface modulus of most saponins significantly increased with the time elapsed after the pre-shear of the layer, t_A (for brevity, we call this period "time of layer aging"). To study the effect of the aging process, we applied continuous oscillations of the adsorption layers for 12 h, at fixed strain amplitude (0.1%) and

constant frequency (1 Hz). These measurements allowed us to monitor the evolution of the viscous and elastic moduli, as functions of aging time, t_A. Control experiments were performed just before and after the long experiments to check for possible effects of water evaporation from the solution surface, which could compromise the results. These control experiments gave the same experimental result, thus confirming that the water evaporation had not affected our data.

3 Results and discussion

3.1 Comparison of the rheological response of adsorption layers from different saponins

To compare the studied saponin extracts, we subjected their adsorption layers to a creep-recovery experiment by applying a torque of 1 μN m for 100 s, after 30 min of layer aging. The obtained results are compared in Fig. 3. One sees that, with regard to the type of rheological response, the saponins can be divided into three groups: (1) the first group includes QD, BSC, TS, Escin and GS. The layers of these saponins exhibit a visco-elastic response with high surface elasticity, and therefore, this group will be denoted hereafter as "Group EV" (EV stands for high Elasticity and Viscosity). (2) The layers from the saponins in the second group, including HC and SAP, show a viscous response with sufficiently high surface viscosity to be measured. Therefore, this group will be denoted as "Group V". For this group, Bo > 100, so we could determine the surface shear viscosity without data corrections. (3) The third group, including FD, FS, TT, ASC, LIC, also shows a viscous response only, but the surface viscosity is very low and Bo < 30. For ASC, FS and FD, the surface deformation was very close to that of a surfactant-free surface, which means negligible surface

viscosity. Therefore, this group will be denoted as "Group LV" to indicate that the respective saponins exhibit negligible surface elasticity and very low viscosity. As we are interested mostly in the systems with high surface modulus, the saponins from Group LV were not studied experimentally any further.

Below, we report results obtained with saponins from Group EV (Sections 3.3 and 3.4) and Group V (Section 3.5). Section 3.6 compares the data obtained in the current study with QD extract to those obtained with other rheometers and geometries from our previous study.[13] In Section 3.7, we trace the relation between the surface rheological behavior of the various saponins and their molecular structures.

3.2 Rheological model describing the response of saponins from Group EV

In our previous study,[13] we showed that the compound Voigt (CV) rheological model describes very well the response of QD visco-elastic adsorption layers. The mechanical analog of this model can be presented as a combination of one Maxwell and two Kelvin elements, connected sequentially – see Fig. 4. As explained in Section 3.2.1 of ref. 13, no simpler rheological model could describe the observed visco-elastic properties of these layers, due to the complex shape of the creep-recovery curves, with two relaxation times clearly visible in the recovery branch of the curves.

According to the CV model, the compliance during creep, J_{CR}, is described by the following equation:

$$J(t) = \frac{1}{G_0} + \frac{1}{G_1}\left[1 - \exp\left(-\frac{t}{\lambda_1}\right)\right] + \frac{1}{G_2}\left[1 - \exp\left(-\frac{t}{\lambda_2}\right)\right] + \frac{t}{\eta_0}$$

(4)
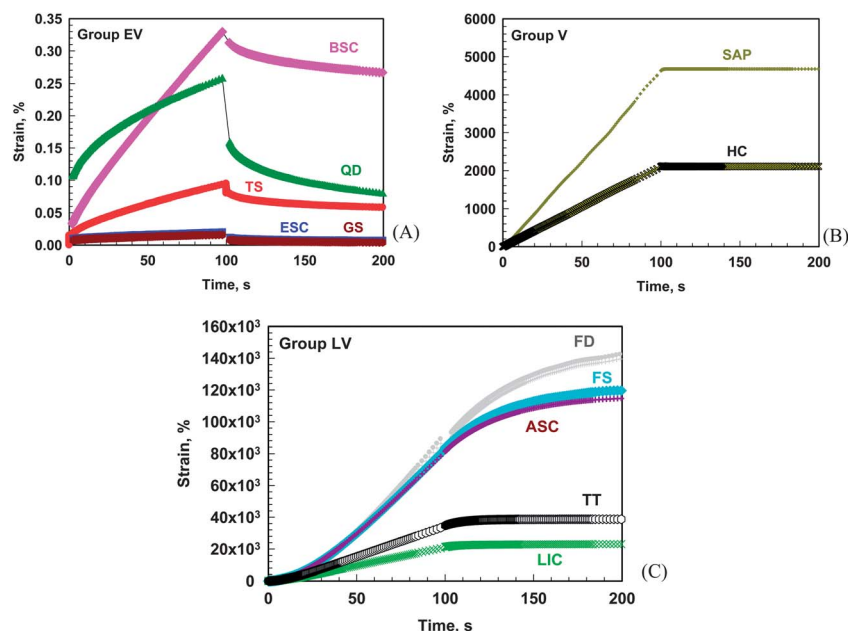
Fig. 3 Creep and relaxation of saponin adsorption layers. t_A = 30 min; t_{CR} = 100 s; torque M = 1 μN m. (A) Group EV of saponins with elasto-viscous properties of the adsorption layers; (B) Group V with measurable surface shear viscosity; and (C) Group LV with very low shear surface viscosity.
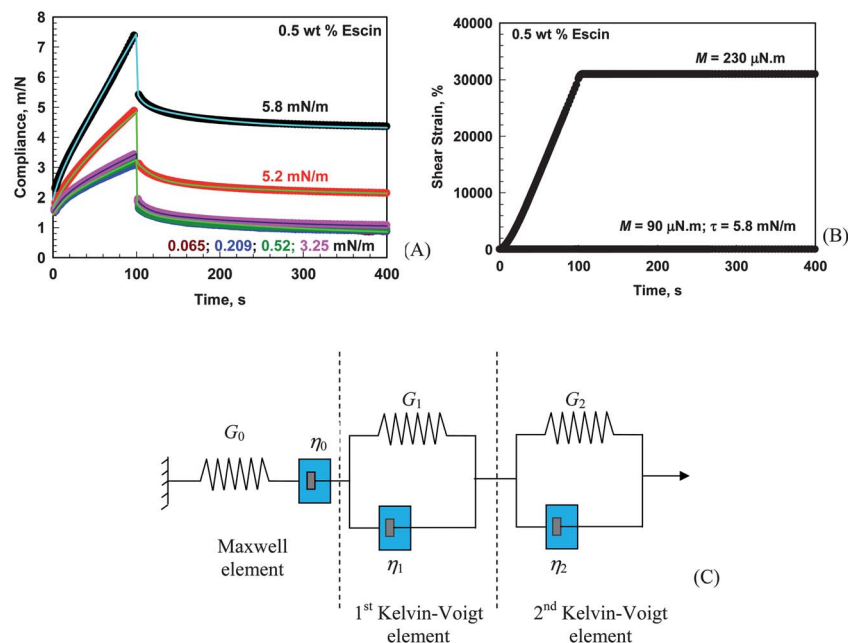
Fig. 4 (A) Creep and relaxation of the adsorption layer of Escin, $t_A = 30$ min; $t_{CR} = 100$ s at $\tau \leq \tau_C$. (B) Shear strain at $\tau \geq \tau_C$. Note that the lower curve here is equivalent to the uppermost curve in (A), except for the changed scale of the ordinate. The solid curves in (A) represent fit with the compound Voigt model, which is schematically shown in (C).

and the recovery is governed by:

$$J_R(t) = \frac{t_{CR}}{\eta_0} + \frac{1}{G_1}\left[1 - \exp\left(-\frac{t_{CR}}{\lambda_1}\right)\right]\exp\left(-\frac{t}{\lambda_1}\right)$$
$$+ \frac{1}{G_2}\left[1 - \exp\left(-\frac{t_{CR}}{\lambda_2}\right)\right]\exp\left(-\frac{t}{\lambda_2}\right) \quad (5)$$

where G_0, η_0 and $\lambda_0 = \eta_0/G_0$ are the elastic modulus, viscosity, and relaxation time of the Maxwell element, respectively, while G_i, η_i and $\lambda_i = \eta_i/G_i$ are the characteristics of the i-th Kelvin element ($i = 1,2$).

3.3 Surface rheological properties of saponin layers from Group EV, as determined from creep-recovery experiments

Experiments with saponin layers aged for 30 min, at surface shear stress between 0.065 mN m^{-1} and 5.8 mN m^{-1}, were performed with layers of the saponins from Group EV (QD, BSC, TS, GS and Escin). For each of these layers, we observed that a single master curve describes the compliance *vs.* time results, obtained at different stresses, when the shear stress is below a given critical value, $\tau < \tau_C$; see for example the data with Escin layers at $\tau \leq 3.25$ mN m^{-1}, shown in Fig. 4A. The value of τ_C depends on the specific saponin sample. At $\tau > \tau_C$, the compliance increases with the increasing applied stress, but the layer may still exhibit strong elasticity, as seen from the results obtained at 5.2 and 5.8 mN m^{-1} in Fig. 4A. At even higher torque (corresponding approximately to $\tau \approx 14.8$ mN m^{-1}, when eqn (3) is used to estimate the stress from the torque), the response of the Escin layers becomes purely viscous; see Fig. 4B. Therefore, the critical shear stress, which leads to fluidization of the Escin layer, is around 10 mN m^{-1} for the 30 min aged layer.

Below in this section, we present experimental results, obtained at $\tau \leq \tau_C$, which were fitted by the CV model for QD, TS, Escin and GS. The relaxation of the BSC adsorption layer showed one relaxation time only, and therefore, the experimental data for this saponin were fitted by the simpler Burgers model (one Maxwell and one Kelvin elements).

The obtained values for the Maxwell and the two Kelvin elements are compared in Fig. 5 for the various saponins with visco-elastic behavior. The obtained results for G_i ($i = 0,1,2$) are compared in Fig. 5A. One sees that G_0 is highest for GS monolayers (≈ 840 mN m^{-1}) and Escin (≈ 660 mN m^{-1}), intermediate for TS (≈ 460 mN m^{-1}) and BSC (≈ 230 mN m^{-1}), and lowest for QD (≈ 58 mN m^{-1}). With respect to G_1, again the highest value was determined for GS and Escin (≈ 2400 mN m^{-1}), around 5 times lower for TS (≈ 440 mN m^{-1}), more than 10 times lower for BSC (≈ 200 mN m^{-1}), and the lowest value was measured with QD again (≈ 100 mN m^{-1}). The values of G_2 for Escin and GS are ≈ 800 mN m^{-1}, for TS ≈ 190 mN m^{-1}, and for QD ≈ 30 mN m^{-1}. Therefore, with respect to the shear elasticities, the largest values are measured with Escin and GS adsorption layers.

The obtained results for the surface shear viscosities are compared in Fig. 5B. One sees that η_0 is largest for GS ≈ 190 Pa s m and Escin ≈ 130 Pa s m, much lower for TS and QD ≈ 10 Pa s m, and lowest for BSC ≈ 2 Pa s m. The values of η_1 are much lower than those of η_0 for all saponins, except for BSC. Comparable values of η_2 and η_0 were determined for GS, Escin and QD. For the TS layer, η_2 is higher than η_0.

As a result of the significant variations of η_0, the relaxation times for the Maxwell element also differ significantly for the various saponins; see Fig. 5C. For GS, QD and Escin, $\lambda_0 \approx 180$ s,
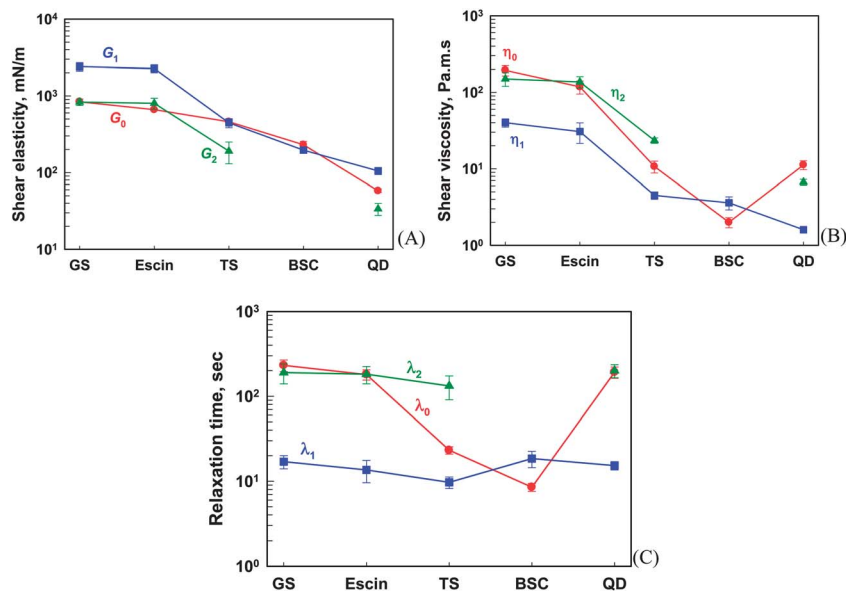
Fig. 5 (A) Surface shear elasticities; (B) surface shear viscosities and (C) relaxation times for Maxwell (index 0) and two Kelvin elements (indexes 1 and 2) as determined from the best fit of the experimental data with the compound Voigt model (for GS, Escin, TS and QD) and the Burgers model for BSC adsorption layers. The data are averaged from at least four experiments, performed at $\tau \leq 3.25$ mN m^{-1} for Escin; ≤ 0.79 mN m^{-1} for BSC; ≤ 0.52 mN m^{-1} for TS and QD, and ≤ 0.21 mN m^{-1} for GS.

whereas it is ≈ 23 s for TS and ≈ 8 s for BSC. Interestingly, the recovery times for the first Kelvin element are between 10 and 18 s for all studied saponins; see Fig. 5C. Similarly, the characteristic recovery times for the second Kelvin element are again very similar, $\lambda_2 \approx 180$ s, for all studied saponins (except for BSC where it is missing). In conclusion, the saponins differ significantly with respect to the relaxation time λ_0 only, whereas no significant difference is observed with respect to λ_1 and λ_2.

Summarizing the main trends, the rheological response of Escin and GS adsorption layers is very similar. These layers are very elastic with $G_0 \approx G_2 \approx 800$ mN m^{-1}, $G_1 \approx 2400$ mN m^{-1} and the characteristic times of $\lambda_0 \approx \lambda_2 \approx 180$ s ($\eta_0 \approx \eta_2 \approx 150$ Pa s m), and $\lambda_1 \approx 15$ s ($\eta_1 \approx 35$ Pa s m). The relaxation times of the QD adsorption layers are very similar to those for Escin and GS, but the values $G_0 \approx G_2 \approx 55$ mN m^{-1} and $\eta_0 \approx \eta_2 \approx 10$ Pa s m are much lower than those for Escin and GS. On the other hand, TS and BSC have much shorter relaxation times for the Maxwell element, $\lambda_0 \approx 23$ s (TS) and 8 s (BSC), and intermediate values of $G_0 \approx 450$ mN m^{-1} (TS) and 240 mN m^{-1} (BSC).

In our previous paper,[13] we assumed that the observed complex rheological behaviour of the saponin adsorption layers is related to their structure, which is probably composed of tightly packed domains, separated by mechanically weaker domain boundaries. On the basis of this assumption, we proposed three molecular mechanisms for relaxation of the distorted domain structure, formed under applied shear stress: (1) sliding of the domains with respect to each other, under the action of the applied stress, which is associated with the relaxation time of the Maxwell element, λ_0; (2) visco-plastic deformation of the domain boundaries, *via* migration of molecules along the domain sides, which is associated with the relaxation time of the first Kelvin element, λ_1; and (3) rearrangement of the molecules inside the domains for restoring

their most favoured intermolecular orientation, so that the energy of molecular interactions inside the domains is minimized. This process is associated with the relaxation time of the second Kelvin element, λ_2. The specific experimental results supporting this interpretation (still speculative at the present moment) and their discussion are presented in ref. 13.

In the current study, we see that λ_1 is ≈ 10–15 s for all studied saponins from Group EV, which suggests that the migration of the molecules along the domain boundaries does not depend significantly on the specific saponins. These "boundary" molecules could be of saponins or of some other extract components, *viz.* surface active contaminants. In contrast, the values of λ_0 and λ_2 depend strongly on the adsorbed saponin. The value of λ_0 is the highest for GS, Escin and QD, and much lower for TS and BSC. These results suggest that the domain sliding is more difficult for GS, Escin and QD, as compared to TS and BSC. This might be due to different shapes of the domains or some other reasons which are not clear at the moment. The values of λ_2 are long and similar for GS, Escin, QD and TS, and missing for BSC. This means that the rearrangement of molecules inside the tightly packed domains of GS, Escin, QD and TS is difficult (as expected), whereas no such process is observed with BSC.

Let us note that the measured elasticities, $G_i \approx 10^3$ mN m^{-1}, and viscosities, $\eta_i \approx 10^2$ N s m^{-1}, are remarkably high. The typical dimensions of the saponin molecules are around 3–5 nm. This layer thickness was estimated by two different methods: (1) from the molecular mass of the saponins, we determined the volume of one molecule (assuming a mass density of ≈ 1 g cm^{-3}). Knowing the area per molecule in the adsorption layer from the surface tension isotherms, we estimated that the thickness of the adsorption layers is between 2.5 and 4.4 nm for the various saponins. (2) By computer modeling, we determined the molecular dimensions of the various

saponin molecules, and by orienting them properly on the interface, we estimated the thickness of the adsorption layer which varied between 2 and 3.5 nm. For approximate estimates, we use below the average value of 3 nm.

The transfer of the surface rheological characteristics into bulk properties of the adsorption layers (by dividing G_i and η_i with the layer thickness) leads to values of the bulk shear elasticity $\approx 10^7$ to 10^8 Pa and bulk shear viscosity $\approx 10^{10}$ Pa s. Although these values are very high, they are physically realistic. For example, the estimated bulk elastic modulus of the saponin layers is comparable to that of the polyethylene plastic material and two-three orders of magnitude lower than that of the typical metals and solid glass.[49] The estimated bulk viscosity is comparable to that of bitumen and is three orders of magnitude lower than that of the solid ice[49] which is also governed by non-covalent hydrogen bonds. Thus, we see that the estimated elasticity and viscosity correspond to those of soft solid materials and, therefore, are not physically unrealistic, despite being several orders of magnitude higher than the typical values, measured with protein and polymer adsorption layers.[50]

The assumption that the interactions between the saponin molecules are most probably governed by hydrogen bonds, and possibly reinforced by hydrophobic interactions, was supported by the experimental observation that the addition of 4 M of the chaotropic agent urea to the aqueous subphase of TS, led to complete disappearance of the high surface elasticity and viscosity of the TS adsorption layer. The chaotropic agents are known to disrupt the water structure and, in this way, to deteriorate almost completely the hydrogen bonds and the hydrophobic interactions.

3.4 Surface rheological properties of saponin layers from Group EV, as determined from oscillatory experiments

3.4.1 Strain amplitude experiments. Fig. 6 compares results for the elastic and viscous moduli of the saponins in Group EV, in the amplitude sweep test. At low strain amplitudes, G' and G'' remain almost constant. At certain strain, the elastic modulus starts decreasing, while the viscous modulus passes through a maximum. Such behavior is observed with various systems in bulk rheology (foams, emulsions, suspensions, polymer solutions, filled polymers, *etc.*) and in surface rheology (low-molecular mass surfactants,[51] proteins,[52] and particles[53]). According to the classification of the behavior at large amplitude oscillatory shear established for bulk rheology,[54] we can classify our systems as weak strain overshoot, where G' decreases with amplitude and G'' shows strain overshoot. The local maximum in G'' is explained as arising from the balance between the formation and the destruction of the network junctions. Depending on the class of the soft material, the explanation for the local maximum is different.[55] Parthasarathy and Klingenberg[56] explained the overshooting with the initial increase of viscous dissipation due to the slight rearrangement of unstable clusters under shear, while the decrease at large strain is associated with large structural changes. This is the most probable explanation for our systems as well. Above a given shear strain G'' starts to increase due to the sliding of the different domains with respect to each other, while the layer structure changes significantly after the maximum in G''.

We can characterize our systems by determining the value of γ_0 at which the G' and G'' start to deviate from their initial values (in the linear regime) and the value of γ_{cr} at the maximum in G'' which corresponds to the strain leading to disruption of the internal structure.

To determine γ_0, where the layer starts to exhibit a non-linear response, we defined the value of γ_0 as the deformation at which G' decreases down to 95% from its initial value.[57] The values of γ_0 for the various samples are compared in Fig. 7A. One sees that the highest critical strain is observed with the layer of QD – this layer can be described by linear viscoelasticity for strains up to 0.8%, whereas a non-linear response appears at $\gamma_0 \approx 0.17\%$ only for GS layers. TS, BSC and Escin layers have intermediate values of γ_0 between 0.4 and 0.6%. The corresponding values of the surface stress, at which the non-linear response appears, are shown by red circles in Fig. 7B. One sees that the highest value is obtained for Escin (≈ 5.5 mN m^{-1}), which is in relatively good agreement with the experimental results, obtained by creep-recovery experiments, where all data obtained at $\tau \leq 3.25$ mN m^{-1} merge on the same graph compliance *vs.* time; see Fig. 4A. We must note that γ_0 and τ_0 were determined with poor reproducibility for ESC. The critical value for QD determined from amplitude sweep experiments is ≈ 0.64 mN m^{-1}, which is also in good agreement with the experimental results, obtained in the creep-recovery experiments described in ref. 13, where all data for $\tau \leq 0.94$ mN m^{-1} were falling on the same compliance curve. For the other saponins, we cannot make such direct comparison because the creep-recovery experiments were performed only at stresses which were below the critical ones.
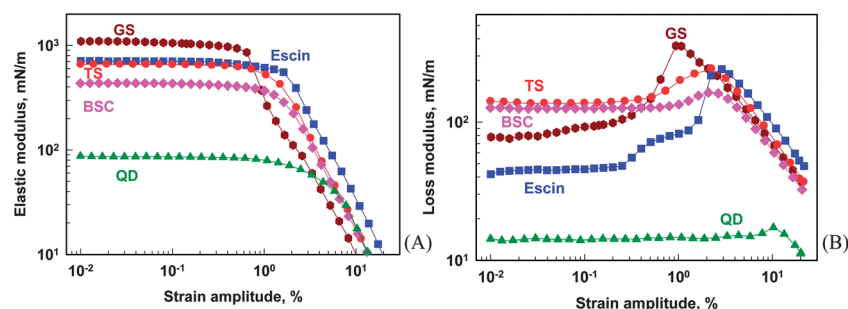
Fig. 6 Elastic and viscous moduli *vs.* strain amplitude at constant frequency (1 Hz). The strain amplitude is varied logarithmically from 0.01 to 20%. The aging time is 30 min.
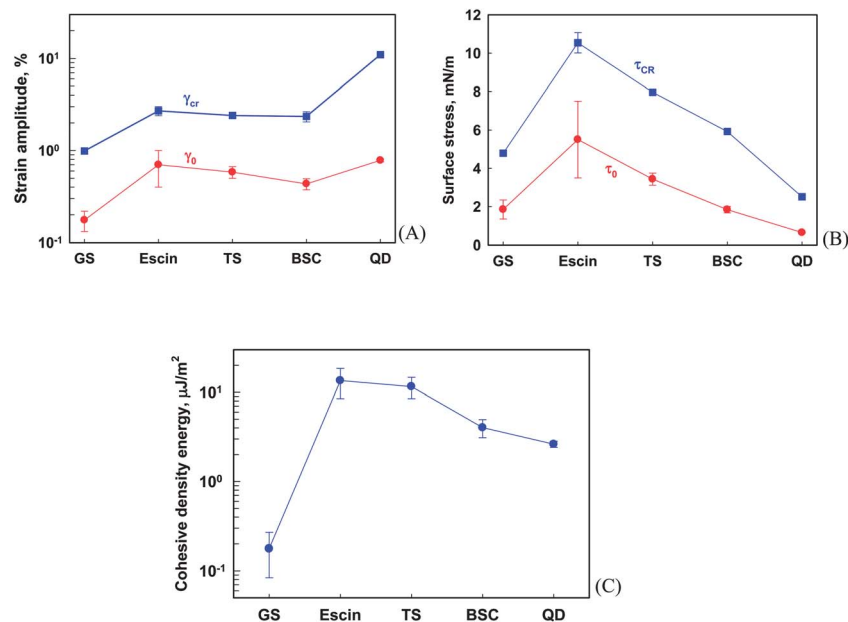
Fig. 7 (A) Strain amplitude at which $G' = 0.95 \, G'$ ($\gamma \to 0$) denoted as γ_0 (red points), and strain amplitude at which the maximum of G'' is observed, denoted as γ_{CR} (blue points) and the respective stresses (B). (C) Cohesive density energy calculated from eqn (6). The data are averaged from at least three experiments.

As a quantitative characteristic of the transition in the internal structure of the layer, leading to its fluidization, we used the strain at which G'' has a maximum (this strain is very similar to the cross-over point $G' = G''$); see the blue points in Fig. 7A and B. One sees that the properties of QD differ significantly, compared to all other saponins in this group. In QD, the internal structure is disrupted at relatively high γ_{CR} ($\approx 11\%$) and low τ_{CR} ($\approx 2.5 \, \text{mN m}^{-1}$). The latter value is in good agreement with the results from the creep-recovery experiments in our previous study,[13] where we found that the internal structure of the QD layer is disturbed heavily at $\tau > 1.8 \, \text{mN m}^{-1}$, and as a result, the layer behaves as a purely viscous body.

Similarly good agreement is observed for the Escin layer – from creep-recovery experiments, we determined that the Escin layer decreases its elastic response at stresses between 3.25 and 5.8 mN m^{-1}, but the internal structure is more or less preserved, whereas at $\tau \approx 14 \, \text{mN m}^{-1}$, the internal structure of the Escin layer is disrupted and the layer is fluidized. Similar conclusions can be drawn on the basis of experimental results from the amplitude sweep experiments, where the critical stress for disruption of the internal structure for the Escin layer is determined to be $\approx 11 \, \text{mN m}^{-1}$. For the other saponins, we determined that the internal structure is preserved up to 8 mN m^{-1} for TS, 6 mN m^{-1} for BSC and 4.8 mN m^{-1} for GS.

An additional characteristic of the elasto-viscous adsorption layers is the cohesive energy density which can be determined from the value of G' in the linear region and γ_0:[58]

$$E_0 = \frac{1}{2} G' \gamma_0^2 \tag{6}$$

Fig. 7C compares the cohesive density energies for the various saponin layers. The highest cohesive energy is

determined for Escin, followed by TS and BSC. An intermediate value is determined for QD, and the lowest value for GS.

In sum, the linear response of QD layers is largest (up to $\approx 0.8\%$), whereas for GS it is the smallest (up to 0.17%). In the linear regime, all layers are elastic. The critical surface stress, above which the layers become fluid, is highest for Escin ($\approx 11 \, \text{mN m}^{-1}$); intermediate for GS, TS and BSC ($\approx 5 \div 8 \, \text{mN m}^{-1}$) and lowest for QD ($\approx 2.5 \, \text{mN m}^{-1}$). The cohesive density energy is highest for TS, intermediate for Escin, BSC and QD, and lowest for GS.

3.4.2 Effect of aging of the adsorption layer on the surface modulus. The change in the surface modulus with the time of layer aging was measured by the procedure described in Section 2.2. In Fig. 8, we present the elastic and viscous moduli, G' and G'', of the saponins in Group EV, as a function of aging time, measured at constant frequency and a strain amplitude of 0.1%. In all systems, we observe a gradual increase of the elastic modulus. For Escin and GS, an overall decrease of the viscous modulus is observed with the aging time, whereas G'' passes through a maximum for TS, BSC and QD. All saponins exhibit very strong elasticity, $G' \gg G''$, and the ratio G'/G'' increases with time.

Although the strain amplitude in this test was very low (0.1%), it is possible that the layer perturbation during the test could affect the kinetics of layer aging. To test this possibility, we performed the following control experiment. The layers of all saponins from Group EV were left to age for 30 min after the pre-shear, without any deformation, and then their surface modulus was measured. In contrast, the results shown in Fig. 8 were obtained by starting the oscillations immediately after the pre-shear. Both procedures gave the same results within the experimental error of the measurement, thus indicating that the used small oscillatory deformations did not interfere with the aging process.
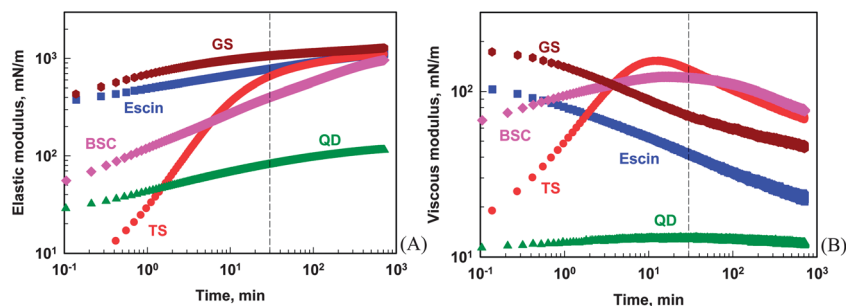
Fig. 8 Surface moduli *vs.* time of aging for saponins from Group EV, at constant frequency (1 Hz), and constant strain amplitude (0.1%). (A) Elastic modulus; (B) viscous modulus.

Aging of saponins with a very long duration for hours or days was observed previously by other authors.[10,15] However, they did not provide information about the used saponins, so that no direct comparison with our results is possible. Very long times for aging were also reported for other surface active species like milk proteins[59] or polysaccharides.[60] The phenomenon is usually explained with the slow kinetics of adsorption, unfolding of the molecules on the interface, and/or formation of intermolecular covalent bonds (disulfide bridges in milk proteins).[61]

Saponins studied here have much lower molecular mass (750 to 2300 g mol^{-1}), M_w, compared to proteins and typical polymers. Some saponins were reported to adsorb relatively slowly on the interface,[9] which could be proposed as a possible reason for the observed slow aging. To check for the importance of this effect, we performed the following control experiment with all saponins from Group EV. The layer was first equilibrated for 1 hour, and then the measurements of G *vs.* t_A started (pre-equilibration + pre-shear + oscillation). In the test used to obtain the results in Fig. 8, the measurements started immediately after pouring the solution in the channel, and positioning the ring on the interface (pre-shear + oscillation). We obtained the same results in these two different types of experiments which is a direct proof that the pre-equilibration step (allowing longer adsorption of the molecules) did not affect the measured values of the surface modulus.

Saponins have not been reported to form specific intermolecular covalent bonds in the adsorption layers (like the milk proteins). However, we cannot exclude completely possible slow reactions inside the adsorption layers, due to the presence of various potentially reacting groups in the saponin molecules (*e.g.*, hydrolysis of the glucoside bonds or ester groups).

In conclusion, a slow aging process is observed for all saponins which is most probably related to a slow rearrangement of the saponin molecules in the adsorption layer at (almost) fixed adsorption. We also cannot completely exclude the possibility of some slow hydrolysis of the glucoside and ester bonds in the adsorbed saponin molecules or even formation of intermolecular covalent bonds inside the adsorption layer, especially at long aging times.

3.5 Surface rheological properties of saponins layers from Group V, as determined from creep-recovery experiments

The samples in Group V are HC and SAP extracts. The adsorption layer of HC behaved like a viscous body during the creep

and recovery tests. The deformation increased linearly during the creep part, and stayed constant during the relaxation part of the experiment; see Fig. 3B. These results were poorly reproducible and the mean value of the surface viscosity was $\approx 0.27 \pm 0.15$ mN s m^{-1} (*i.e.* the surface viscosity varied between *ca.* 0.1 and 0.4 mN s m^{-1} in the various measurements). The HC extract contains Escin as the main saponin component, which in pure form adsorbs in layers with very high surface shear elasticity – see Fig. 5 and 6. This qualitative difference between the surface rheological properties of the pure saponin (Escin) and the related crude plant extract (HC) evidences for the strong effect of the other surface-active substances in the HC extract, which probably inhibit the formation of structured adsorption layer with high surface elasticity (observed with Escin). Note that no such strong effect of the other components was seen with the crude Quillaja extract (QD) and the respective purified saponin (Supersap) whose properties were compared in ref. 13 and very similar surface behavior was observed.

Fig. 9 compares the compliance *vs.* time for deformation for SAP and BSC, at two values of the shear stress, 0.065 and 0.13 mN m^{-1}. As seen from Fig. 9, the SAP layer had a purely viscous behavior with measurable viscosity ($\eta_\text{S} \approx 0.15$ mN s m^{-1}) which places this extract in Group V. In contrast, BSC exhibited high elasticity and viscosity – therefore, it falls in Group EV, as discussed in the preceding sections. The observed qualitative difference between SAP and BSC extracts is noteworthy, because
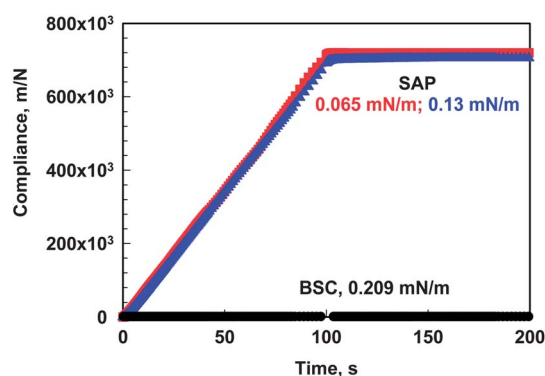
Fig. 9 Compliance *vs.* time during creep and relaxation, for SAP ($\tau = 0.065$ and 0.13 mN m^{-1}) and BSC ($\tau = 0.209$ mN m^{-1}), $t_\text{CR} = 100$ s. The curve for BSC is better seen in Fig. 2 where the same data are shown on the expanded compliance axis.

SAP is extracted from the species *Sapindus trifoliatus* and BSC is extracted from the fruits of a similar plant – *Sapindus mukurrosi*. Previous studies[34] showed that the extracts from these plants contain structurally similar monodesmosidic saponins with oleanane aglycone. Two basic explanations could be proposed for the qualitatively different behavior of these structurally similar saponin molecules: (1) the SAP saponins do not form an elastic adsorption layer on the surface, due to specifics in their molecular structure (*e.g.*, different sugar chains in length and/or composition). (2) SAP has the potential of forming visco-elastic layer, as BSC does, but there are other surface active molecules which lower the surface modulus (as in the case with HC discussed above). A much more complex study, including efforts to separate and purify the main components in the crude extracts, would be needed to clarify which of the above explanations is the real one.

3.6 Comparison between the experimental results obtained in the current study and those described in ref. 13

In our previous study,[13] we measured the surface rheological properties of QD adsorption layers after different times of aging by using a bicone tool attached to a Gemini rheometer. In ref. 13, we observed that the characteristics of the adsorption layers did not change significantly after 5 min of layer aging, and therefore, most of the experiments described in ref. 13 were performed after 5 min of layer aging. However, in the current study performed with DWRG, the aging of QD adsorption layers continued for more than 12 h; see Fig. 8. In both series of experiments, the same batch sample was used and the saponin concentration was 0.5 wt%. The reason for the absence of long-term aging, as measured with the Bohlin rheometer in ref. 13, is not clear at the moment. One possible explanation for the observed difference in the aging evolution of the layers is the presence of some small mechanical disturbances of the adsorption layer in the experiments with the bicone tool, which could prevent the layer from forming a long-term structure and the related aging.

To compare quantitatively the results described in ref. 13 and in the current study, we performed additional experiments with QD layers in the DWRG equipment at 5 min of layer aging. The obtained results are compared in Table 2. First, one sees that both instruments gave very similar values for all relaxation times – the values of λ_i agree in the frame of the experimental error. Also, the values of G_0 and η_0 (Maxwell element) determined by the two instruments are very close. The comparison of the parameters of the Kelvin elements is somewhat worse (around 2 times higher for DWRG), the differences being slightly higher for the second Kelvin element. These differences could be related to more pronounced inertia effects in the bicone tool.

The results in Table 2 also show that there is a gradual increase of all viscous and elastic parameters (η_i, G_i) with aging time, consistent with the increase of surface modulus shown in Fig. 8. The value of λ_0 also increases strongly with aging time, while the values of λ_1 and λ_2 increase slightly only after very long aging times, $t_A = 12$ h.

Table 2 Rheological parameters (compound Voigt model) describing the behavior of an adsorption layer of QD ($t_A = 5$ min), as determined in this work (DWRG) and in ref. 13 (bicone tool)

Parameter	Ref. 13	Current work		
t_A	5 min	5 min	30 min	12 hours
G_0, mN m^{-1}	32 ± 5	38 ± 2	65 ± 1	101 ± 5
η_0, N s m^{-1}	2.0 ± 1.0	2.2 ± 0.1	11.3 ± 1.5	128 ± 28
G_1, mN m^{-1}	31 ± 6	50 ± 8	135 ± 20	335 ± 7
G_2, mN m^{-1}	7 ± 3	18 ± 4	50 ± 10	105 ± 4
η_1, N s m^{-1}	0.3 ± 0.1	0.6 ± 0.1	1.8 ± 0.2	6.0 ± 0.5
η_2, N s m^{-1}	1.3 ± 0.3	3.0 ± 0.3	7.4 ± 0.6	24 ± 3
λ_0, s	43 ± 17	58 ± 2	172 ± 25	1283 ± 354
λ_1, s	10 ± 3	12 ± 1	13 ± 3	17 ± 2
λ_2, s	200 ± 90	170 ± 20	160 ± 50	225 ± 25

In summary, the results with QD at 5 min of layer aging are similar in the two series of measurements; however, there is additional strengthening of the layer when the measurements are made with the double-wall-ring geometry. The reasons for this difference are still not clear, though a possible explanation was proposed above.

3.7 Possible relation between molecular structure and surface rheological properties of triterpenoid saponins

Establishing some common structural features of the molecules in each rheological group (EV, V or LV) would clarify how the molecular structure could affect the rheological behavior of the saponin adsorption layers.

All saponins in Groups EV and V, with relatively high surface moduli, had a triterpenoid type of aglycone (oleanane or dammarane). In contrast, all of the steroid saponins (furastanols or spirostanols) had no surface elasticity and exhibited very low surface viscosity.

Let us first consider the saponins in Group EV which are all of triterpenoid type, with oleanane aglycone, except for GS which has triterpenoid dammarane aglycone. The fact that these saponins exhibit qualitatively similar visco-elastic behavior, despite the significant differences in their specific composition and origin, indicates that the triterpenoid aglycones probably promote denser packing and formation of strong inter-molecular bonds in the adsorption layers, leading to high surface elasticity.

Fig. 8 shows that four saponins from this group (ESC, TS, BSC and GS) reach very similar high values of the elastic modulus after 12 hours of aging. Compared to them, QD has around 8–10 times lower modulus. To explain the difference between QD and the other saponins in Group EV, we have to analyze the structural differences between the respective saponin molecules. Let us first note that in our previous study, we compared the surface properties of the Quillaja Dry (QD) extract with ultrapure Quillaja saponins (Supersap) and showed that the saponins are the key components in the QD extract, governing its surface properties.[13] Therefore, the presence of other, non-saponin surface active components cannot explain the difference between QD and the other saponins in Group EV.

QD contains a mixture of mostly bidesmosidic saponins, with one of the chains having at least 2, and the other one – at least 3 sugar residues. In contrast, ESC is a monodesmosidic saponin, having one sugar chain with 3 residues. The TS extract contains mainly monodesmosidic molecules, while BSC is a mixture of molecules with one or two oligosaccharide chains, with lengths ranging from 2 to 5 residues. Thus, we see that the saponin extracts in Group EV, which exhibit a very high surface modulus, contain monodesmosidic oleanane saponins (except for GS which is a bidesmosidic dammarane saponin). As the monodesmosidic saponins contain a lower number of sugar residues, these saponins are less soluble and more surface-active, compared to the bidesmosides. Probably, the mono-desmosidic saponins pack better at the interface, whereas the bidesmosidic and especially the tridesmosidic saponins form less compact adsorption layers, because the bulky sugar residues disturb the molecular packing (unless the sugar chains are small and/or properly oriented in the layer). This hypothesis is supported by the area per molecule, determined from the surface tension isotherms of the different saponins[62] – we found that the monodesmosides have a considerably lower area per molecule ($A \approx 0.3 \div 0.4$ nm^2), compared to the molecules with two sugar chains ($A \approx 1$ nm^2) – see Fig. 2.

GS has a different type of aglycone (dammarane) from the rest of the saponins in Group EV. The predominant fraction of the saponins in GS has 2 oligosaccharide chains which are rather short – each contains 2 sugar residues. As we do not have results with other saponins having the same aglycone, it is impossible to make definitive conclusions about the structure–performance relation for this type of saponins. We note, however, that the area per molecules for GS is also relatively small (0.32 nm^2) and close to the one of monodesmosidic tri-terpenoids. This again is an indication for better packing of the GS molecules on the surface.

Group V contains HC and SAP which show a relatively high shear surface viscosity, but no layer elasticity. As explained in Section 3.5, the main saponin molecules in HC and SAP are of monodesmosidic triterpenoid type and resemble those in Escin and BSC, respectively (the latter two belonging to Group EV). The most probable explanation for this behavior of HC and SAP is that the other components in these crude extracts prevent the formation of packed elastic layers by the main saponin molecules. Therefore, we expect that properly purified extracts of HC and SAP might be able to form strong elastic layers, similar to those in Group EV. In fact, Escin is such an example of a puri-fied HC component forming highly elastic layers.

Group LV contains three steroid saponins (FD, FS and TT) and two triterpenoid saponins (ASC, LIC) which all make layers with negligible surface shear viscosity and elasticity. Although the statistics of just three steroid saponins is small, the obtained results indicate that the steroid saponins are more prone to form non-elastic layers with low viscosity.

The triterpenoid saponins in Group LV are more intriguing, because ASC and LIC both have an aglycone of oleanane type, as most of the saponins in Group EV. As known from the literature, the water-soluble fraction of the saponins in the ASC extract contains a mixture of bi- and tridesmosidic molecules.[38–40]

Thus, we could explain the properties of ASC as a result of the excessive sugar chains which may disturb the packing in the adsorption layer – see Fig. 2. LIC is in the other end of the solubility spectrum – this is a pure monodesmosidic saponin (a single compound), with a rather short sugar chain (2 residues) and very low solubility in water. As a result of this low solubility, the surface tension of LIC solution is much higher, ≈ 55 mN m^{-1}, compared to the other saponins, ≈ 40 mN m^{-1}. Therefore, the low surface modulus of LIC solutions can be attributed to the very low solubility of this particular saponin and the lack of sufficient molecules to form a packed adsorption layer.

4 Main results and conclusions

In this article, we study the rheological properties of adsorption layers of 8 triterpenoid and 3 steroid saponins at the air–water interface, subject to creep and oscillatory shear deformations. We observed that the adsorption layers of all steroid saponins had no elastic properties and showed very low surface viscosity. In contrast, most of the triterpenoid saponins had visco-elastic properties with high surface elasticity and measurable surface viscosity.

The main features of the visco-elastic rheological response of the triterpenoid saponins can be summarized as follows:

• These layers exhibit remarkably high surface shear elas-ticity and viscosity (up to 1100 mN m^{-1} and 130 N s m^{-1}, respectively). Though unusually high, these values are physi-cally realistic, as discussed in Section 3.3. These values indicate densely packed adsorption layers with very strong intermolec-ular bonds – most probably these are multiple hydrogen bonds between the neighboring sugar fragments of the adsorbed molecules.

• The layers exhibited much higher surface elasticity than viscosity ($G' \gg G''$). The ratio G'/G'' increased with the time of layer aging and, after 12 h, the lowest ratio was $G'/G'' \approx 10$ (Quillaja extract) and the highest was $G'/G'' \approx 50$ (Escin).

• In the amplitude sweep test, G' and G'' stayed constant at low amplitudes. At higher amplitudes, G' decreased and G'' went through a maximum, reflecting the breakage of the inter-molecular bonds and molecular re-arrangement in the adsorption layer.

• At relatively low shear stress, the compliance did not depend on the shear stress, evidencing for the preserved layer structure at small deformations. The rheological response for all these systems was described well by the compound Voigt model, with the exception of BSC which was described by the simpler Burgers model.

• On increasing the shear stress above a certain critical value, the compliance increased with τ, indicating disruption of the layer structure. At even higher stress, the elastic properties of the layers disappeared and the layers behaved as purely viscous. The critical values of τ for layer disruption determined from creep-recovery and large amplitude oscillation experiments are in good agreement with each other.

With respect to the relation between the rheological behavior of the saponin layers and their molecular structure, we could draw the following conclusions:

● All steroid saponins studied by us and by other authors[11] showed no elastic properties and low surface viscosity of their adsorption layers.

● All saponins which exhibited surface shear elasticity were with triterpenoid aglycone of oleanane or dammarane type, with one chain having at least 3 sugar residues or two short oligosaccharide chains. The observed surface elasticity was attributed to the better packing of the molecules in the adsorption layers.

● Four of the triterpenoid samples had no surface elasticity. For two of them, showing negligible surface viscosity, this was attributed to their specific molecular structure: LIC has too short a hydrophilic chain which leads to very low solubility in water, while ASC is a tridesmosidic saponin with excess sugar chains which probably disturbs the molecular packing in the adsorption layers. The other two samples (HC and SAP) had significant surface viscosity, and our results suggest that other surface active molecules, present in these extracts, inhibit the formation of well-packed visco-elastic adsorption layers.

The current study should be considered as an important initial step in revealing the general relations between the molecular structure and the surface rheological properties of various saponins. Further experiments with additional extracts (especially purified ones) are needed to widen the data base and to check critically the hypotheses formulated in the current study.

Acknowledgements

References

1 K. Hostettmann and A. Marston, *Saponins*, Cambridge University Press, New York, 1995.

2 J.-P. Vincken, L. Heng, A. De Groot and H. Gruppen, Saponins, classification and occurrence in the plant kingdom, *Phytochemistry*, 2007, **68**, 275–297.

3 Q. Guglu-Ustundag and G. Mazza, Saponins: Properties, applications and processing, *Crit. Rev. Food Sci. Nutr.*, 2007, **47**, 231–258.

4 C. R. Sirtori, Aescin: Pharmacology, Pharmacokinetics, and Therapeutic Profile, *Pharmacol. Res.*, 2001, **44**, 183–193.

5 M. Miyakoshi, Y. Tamura, H. Masuda, K. Mizutani, O. Tanaka and T. Ikeda, Antiyeast Steroidal Saponins from *Yucca schidigera* (Mohave yucca), a New Anti-Food Deteriorating Agent, *J. Nat. Prod.*, 2000, **63**, 332–338.

6 D. Oakenfull, Soy protein, saponins and plasma cholesterol, *J. Nutr.*, 2001, **131**, 2971–2972.

7 H. R. Shin, J. Y. Kim, T. K. Yun, G. Morgan and H. Vainio, The cancer-preventive potential of *Panax ginseng*: a review of human and experimental evidence, *Cancer, Causes Control, Pap. Symp.*, 2000, **11**, 565–576.

8 C. R. Kensil, A. X. Mo and A. Truneh, Current vaccine adjuvants: an overview of a diverse class, *Front. Biosci.*, 2004, **9**, 2972–2988.

9 R. Stanimirova, K. Marinova, S. Tcholakova, N. D. Denkov, S. Stoyanov and E. Pelan, Surface Rheology of Saponin Adsoprtion Layers, *Langmuir*, 2011, **27**, 12486–12498.

10 S. A. Shorter, On Surface Separation from Solutions of Saponin Peptone, and Albumin, *Phil. Mag.*, 1909, **17**, 560–563.

11 P. Joos, R. Vochten and R. Ruyssen, The Surface Shear Viscosity of Mixed Monolayers Interaction Between Cholesterol and Digitonin, *Bull. Soc. Chim. Belg.*, 1967, **76**, 601.

12 T. B. J. Blijdenstein, P. W. N. de Groot and S. D. Stoyanov, On the link between foam coarsening and surface rheology: Why hydrophobins are so different, *Soft Matter*, 2010, **6**, 1799–1808.

13 K. Golemanov, S. Tcholakova, N. D. Denkov, E. Pelan and S. Stoyanov, Surface shear rheology of saponins, *Langmuir*, 2012, **28**, 12071–12084.

14 M. Piotrowski, J. Lewandowska and K. Wojciechowski, Biosurfactant–protein mixtures: Quillaja Bark Saponin at water/air and water/oil interfaces in presence of β-lactoglobulin, *J. Phys. Chem. B*, 2012, **116**, 4843–4850.

15 J. R. Van Wazer, Some rheological measurements on the surface of saponin in water, *J. Colloid Sci.*, 1947, **2**, 223.

16 N. D. Denkov, S. Tcholakova, K. Golemanov, K. P. Ananthapadmanabhan and A. Lips, The role of surfactant type and bubble surface mobility in foam rheology, *Soft Matter*, 2009, **5**, 3389–3408.

17 A. Saint-Jalmes, Physical chemistry in foam drainage and coarsening, *Soft Matter*, 2006, **2**, 836–849.

18 K. Golemanov, N. D. Denkov, S. Tcholakova, M. Vethamuthu and A. Lips, Surfactant mixtures for control of bubble surface mobility in foam studies, *Langmuir*, 2008, **24**, 9956–9961.

19 S. Tcholakova, Z. Mitrinova, K. Golemanov, N. D. Denkov, M. Vethamuthu and K. P. Ananthpadmanabhan, Control of bubble Ostwald ripening in foams by using surfactant mixtures, *Langmuir*, 2011, **27**, 14807–14819.

20 S. A. Koehler, S. Hilgenfeldt, E. R. Weeks and H. A. Stone, Drainage of single Plateau borders: Direct observation of rigid and mobile interfaces, *Phys. Rev. E: Stat., Nonlinear, Soft Matter Phys.*, 2002, **66**, 040601/1–040601/4.

21 D. Georgieva, A. Cagna and D. Langevin, Link between surface elasticity and foam stability, *Soft Matter*, 2009, **5**, 2063–2071.

22 A. Bhattacharyya, M. Francisco, D. Langevin and J.-F. Argillier, Surface Rheology and Foam Stability of Mixed Surfactant–Polyelectrolyte Solutions, *Langmuir*, 2000, **16**, 8727–8732.

23 S. Marze, D. Langevin and A. Saint-Jalmes, Aqueous foam slip and shear regimes determined by rheometry and multiple light scattering, *J. Rheol.*, 2008, **52**, 1091–1111.

24 M. Durand and H. Stone, Relaxation time for the topological T1 process in a two-dimensional foam, *Phys. Rev. Lett.*, 2006, **97**, 226101.

25 S. Cohen-Addad, R. Hohler and Y. Khidas, Origin of the slow linear viscoleastic response of aqueous foams, *Phys. Rev. Lett.*, 2004, **93**, 028302–028311.

26 T. B. J. Blijdenstein, R. Ganzevles, P. W. N. de Groot and S. D. Stoyanov, On the link between surface rheology and foam disproportionation in mixed hydrophobin HFBII and whey protein systems, *Colloids Surf., A*, 2012, DOI: 10.1016/j.colsurfa.2012.12.040.

27 K. D. Danov, G. M. Radulova, P. A. Kralchevsky, K. Golemanov and S. D. Stoyanov, Surface shear rheology of hydrophobin adsorption layers: laws of viscoelastic behaviour with applications to long-term foam stability, *Faraday Discuss.*, 2012, **158**, 195–221.

28 H. Jin, W. Zhou, J. Cao, S. D. Stoyanov, T. B. J. Blijdenstein, P. W. N. de Groot and E. G. Pelan, Super Stable Foams Using Ethyl Cellulose Colloidal Particles, *Soft Matter*, 2012, **8**, 2194–2205.

29 R. D. Groot and S. D. Stoyanov, Close packing density and fracture strength of adsorbed polydisperse particle layers, *Soft Matter*, 2011, **7**, 4750–4761.

30 B. S. Murray, K. Durga, A. Yusoff and S. D. Stoyanov, Stabilization of foams and emulsions by mixtures of surface active food-grade particles and proteins, *Food Hydrocolloids*, 2011, **25**, 627–638.

31 Y. Shimizu and S. W. Pelletier, Elucidation of the Structures of the Sapogenins of *Polygala senega* by Correlation with Medicagenic Acid, *J. Am. Chem. Soc.*, 1966, **88**, 1544.

32 J. Yan, Z. Wu, Y. Zhao and C. Jiang, Separation of tea saponin by two-stage foam fractionation, *Sep. Purif. Technol.*, 2011, **80**, 300–305.

33 B. N. Suhagia, I. S. Rathod and S. Sindhu, *Sapindus mukorossi* (areetha): an overview, *Int. J. Pharma Sci. Res.*, 2011, **2**(8), 1905–1913.

34 R. K. Grover, A. D. Roy, R. Roy, S. K. Joshi, V. Srivastava and S. K. Arora, Complete ^{1}H and ^{13}C NMR assignments of six saponins from *Sapindus trifoliatus*, *Magn. Reson. Chem.*, 2005, **43**, 1072–1076.

35 J. Bankefors, L. I. Nord and L. Lennart Kenne, Structural classification of Quillaja saponins by electrospray ionization ion trap multiple-stage mass spectrometry in combination with multivariate analysis, proof of concept, *Chemom. Intell. Lab. Syst.*, 2008, **90**, 178–187.

36 B. E. Asafu-adjaye and S. K. Wong, Determination of Ginsenosides (Ginseng Saponins) in Dry Root Powder from *Panax ginseng*, *Panax quinquefolius*, and Selected Commercial Products by Liquid Chromatography: Interlaboratory Study, *J. AOAC Int.*, 2003, **86**, 1112–1123.

37 H. Yamaguchi, H. Matsuura, R. Kasai, O. Tanaka, M. Satake, H. Kohda, H. Izumi, M. Nuno, S. Katsuki, S. Isoda, J. Shoji and K. Goto, Analysis of Saponins of Wild *Panax ginseng*, *Chem. Pharm. Bull.*, 1988, **36**, 4177–4181.

38 M. Abul Gafur, T. Obata, F. Kiuchi and Y. Tsuda, *Acacia concinna* saponins. I. Structures of prosapogenols, concinnosides A–F, isolated from the alkaline hydrolysate of the highly polar saponin fraction, *Chem. Pharm. Bull.*, 1997, **45**, 620–625.

39 F. Kiuchi, M. Abul Gafur, T. Obata, A. Tachibana and Y. Tsuda, *Acaciaconcinna* Saponins. II. Structures of Monoterpenoid Glycosides in the Alkaline Hydrolysate of the Saponin Fraction, *Chem. Pharm. Bull.*, 1997, **45**, 807–812.

40 Y. Tezuka, K. Honda, A. H. Banskota, M. M. Thet and K. Shigetoshi, Kinmoonosides A–C, Three New Cytotoxic Saponins from the Fruits of *Acacia concinna*, a Medicinal Plant Collected in Myanmar, *J. Nat. Prod.*, 2000, **63**, 1658–1664.

41 D. Dinchev, B. Janda, L. Evstatieva, W. Oleszek, W. R. Aslani and I. Kostova, Distribution of steroidal saponins in *Tribulus terrestris* from different geographical regions, *Phytochemistry*, 2008, **69**, 176–186.

42 W. Yan, K. Ohtani, R. Kasai and K. Yamasaki, Steroidal saponins from fruits of *Tribulus terrestris*, *Phytochemistry*, 1996, **42**, 1417–1422.

43 W. Oleszek, M. Sitek, A. Stochmal, S. Piacente, C. Pizza and P. Cheeke, Steroidal Saponins of *Yucca schidigera* Roezl, *J. Agric. Food Chem.*, 2001, **49**, 4392–4396.

44 P. R. Petit, Y. D. Sauvaire, D. M. Hillaire-Buys, O. M. Leconte, Y. G. Baissac, G. R. Ponsin and G. R. Ribes, Steroid saponins from fenugreek seeds: Extraction, purification, and pharmacological investigation on feeding behavior and plasma cholesterol, *Steroids*, 1995, **60**, 674–680.

45 M. Yoshikawa, T. Murakami, H. Komatsu, N. Murakami, J. Yamahara and H. Matsuda, Medicinal foodstuffs. IV. Fenugreek seed. (1): structures of trigoneosides Ia, Ib, IIa, IIb, IIIa, and IIIb, new furostanol saponins from the seeds of Indian *Trigonella foenum-graecum* L., *Chem. Pharm. Bull.*, 1997, **45**, 81–87.

46 S. Vandebril, A. Franc, G. G. Fuller, P. Moldenaers and J. Vermant, A double wall-ring geometry for interfacial shear rheometry, *Rheol. Acta*, 2010, **49**, 131–144.

47 A. Franck, S. Vandebril, J. Vermant and G. Fuller, Double wall ring geometry to measure interfacial rheological properties, 5th International Symposium on Food Rheology and Structure, Zurich, Switzerland, 2008.

48 D. A. Edwards, H. Brenner and D. T. Wasan, *Interfacial Transport Processes and Rheology*, Butterworth-Heinemann, Boston, 1991.

49 H. Barnes, *A Handbook of Elementary Rheology*, The University of Wales Institute of Non-Newtonian Fluid Mechanics, Department of Mathematics, University of Wales Aberystwyth, Penglais, Aberystwyth, Dyfed, Wales, SY23 3BZ, 2000.

50 A. Maestro, L. J. Bonales, H. Ritacco, T. M. Fischer, R. G. Rubio and F. Ortega, Surface rheology: macro- and microrheology of poly(*tert*-butyl acrylate) monolayers, *Soft Matter*, 2011, **7**, 7761–7771.

51 R. Krishnaswamy, S. Majumdar and A. K. Sood, Nonlinear Viscoelasticity of Sorbitan Tristearate Monolayers at Liquid/Gas Interface, *Langmuir*, 2007, **23**, 12951–12958.

52 A. Torcello-Gomez, J. Maldonado-Valderrama, M. J. Galvez-Ruiz, A. Martin-Rodriguez, M. A. Cabrerizo-Vilchez and J. de Vicente, Surface rheology of sorbitan tristearate and b-lactoglobulin: Shear and dilatational behavior, *J. Non-Newtonian Fluid Mech.*, 2011, **166**, 713–722.

53 D. Zang, D. Langevin, B. P. Binks and B. Wei, Shearing particle monolayers: Strain-rate frequency superposition, *Phys. Rev. E: Stat., Nonlinear, Soft Matter Phys.*, 2010, **81**, 011604.

54 K. Hyun, S. H. Kim, K. H. Ahn and S. J. Lee, Large amplitude oscillatory shear as a way to classify the complex fluids, *J. Non-Newtonian Fluid Mech.*, 2002, **107**, 51–65.

55 K. Hyun, M. Wilhelm, C. O. Klein, K. S. Cho, J. G. Nam, K. H. Ahn, S. J. Lee, R. H. Ewoldt and G. H. McKinley, A review of nonlinear oscillatory shear tests: Analysis and application of large amplitude oscillatory shear (LAOS), *Prog. Polym. Sci.*, 2011, **36**, 1697–1753.

56 M. Parthasarathy and D. J. Klingenberg, Large amplitude oscillatory shear of ER suspensions, *J. Non-Newtonian Fluid Mech.*, 1999, **81**, 83–104.

57 T. G. Mezger, *The Rheology Handbook*, 2nd ed, Vincentz Network, Hannover, 2006.

58 T. F. Tadros, Rheology of Dispersions: Principles and Applications, Wiley-VCH Verlag GmBH & Co. KGaA, Weinheim, 2010.

59 E. M. Freer, K. S. Yim, G. G. Fuller and C. J. Radke, Interfacial Rheology of Globular and Flexible Proteins at the Hexadecane/Water Interface: Comparison of Shear and Dilatation Deformation, *J. Phys. Chem. B*, 2004, **108**, 3835–3844.

60 P. Erni, E. J. Windhab, R. Gunde, M. Graber, B. Pfister, A. Parker and P. Fischer, Interfacial Rheology of Surface-Active Biopolymers: Acacia, *Biomacromolecules*, 2007, **8**, 3458–3466.

61 E. Dickinson and Y. Matsumura, Time-dependent polymerization of β-Lactoglobulin through disulfide bonds at the oil–water interface in emulsions, *Int. J. Biol. Macromol.*, 1991, **13**, 26–30.

62 K. Golemanov, S. Tcholakova, N. Denkov, E. D. Pelan and S. D. Stoyanov, Dilatational surface rheology of triterpenoid and steroid saponins at the air–water interface, *Langmuir*, 2013, in preparation.